Journal of Hazardous Materials 192 (2011) 124–130

Contents lists available at ScienceDirect

Journal of Hazardous Materials

journal homepage: www.elsevier.com/locate/jhazmat

# Simultaneous absorption of $NO_x$ and $SO_2$ from flue gas with pyrolusite slurry combined with gas-phase oxidation of NO using ozone

Sun Wei-yi, Ding Sang-lan, Zeng Shan-shan, Su Shi-jun*, Jiang Wen-ju

*Department of Environmental Science and Engineering, Sichuan University, Chengdu 610065, China*

ARTICLE INFO

*Article history:*
Received 27 January 2011
Received in revised form 27 April 2011
Accepted 28 April 2011
Available online 5 May 2011

*Keywords:*
Ozone
Pyrolusite slurry
Simultaneous absorption of $NO_x$ and $SO_2$
Manganese sulphate
Manganese nitrate

ABSTRACT

NO was oxidized into $NO_2$ first by injecting ozone into flue gas stream, and then $NO_2$ was absorbed from flue gas simultaneously with $SO_2$ by pyrolusite slurry. Reaction mechanism and products during the absorption process were discussed in the followings. Effects of concentrations of injected ozone, inlet NO, pyrolusite and reaction temperature on $NO_x/SO_2$ removal efficiency and Mn extraction rate were also investigated. The results showed that ozone could oxidize NO to $NO_2$ with selectivity and high efficiency, furthermore, $MnO_2$ in pyrolusite slurry could oxidize $SO_2$ and $NO_2$ into $MnSO_4$ and $Mn(NO_3)_2$ in liquid phase, respectively. Temperature and concentrations of injected ozone and inlet NO had little impact on both $SO_2$ removal efficiency and Mn extraction rate. Specifically, Mn extraction rate remained steady at around 85% when $SO_2$ removal efficiency dropped to 90%. $NO_x$ removal efficiency increased with the increasing of ozone concentration, inlet NO concentration and pyrolusite concentration, however, it remained stable when reaction temperature increased from 20 °C to 40 °C and decreased when the flue gas temperature exceeded 40 °C. $NO_x$ removal efficiency reached 82% when inlet NO at 750 ppm, injected ozone at 900 ppm, concentration of pyrolusite at 500 g/L and temperature at 25 °C.



## 1. Introduction

Due to the fact that $SO_2$ is a key contributor to "acid rain" [1] and $NO_x$ also contributes considerably to both "acid rain" [1] and "greenhouse effect" [2], emissions of $SO_2$ and $NO_x$, mainly from combustion of coal and fuel oils, have brought about significant effects on both environment and human health [3]. Various kinds of technologies have been developed to control and reduce $SO_2$ and $NO_x$ emissions worldwide. Though high $SO_2$ removal efficiency can be obtained by wet $SO_2$ removal process which is widely used at present, it is difficult to attain the high $NO_x$ removal efficiency at the same time because of the low solubility of NO that accounts for more than 90% of all $NO_x$ [4,5]. Moreover, the presence of $SO_2$ can also lead to catalyst poisoned and invalidation in selective catalytic reduction (SCR) process [6,7], which is considered as the most effective process for $NO_x$ removal. Hence, currently a relatively mature solution for removing $SO_2$ and $NO_x$ is referred as an integrated set-up consisting of wet process for $SO_2$ removal and selective catalytic reduction (SCR) for $NO_x$ removal. The two independent systems can remove $SO_2$ and $NO_x$ step by step with high efficiency, but with drawbacks such as large areas, complex system, high investment and operation cost [7–9]. In order to overcome above-mentioned problems, a large number of strong oxidizing agents are added into $NO_x$ removal process [10–21] to obtain the satisfying $NO_x$ removal efficiency as $SO_2$ in wet process. These approaches are divided into absorption–oxidation process [2,10–14] and oxidation–absorption process [8,15–21]. In absorption–oxidation process, liquid oxidants with strong oxidability are used as absorbent, such as sodium chlorite [10–12], hydrogen peroxide [13] and potassium permanganate [2,14]. Although using strong oxidizing agents can improve $NO_x$ removal efficiency, there are certain drawbacks, such as the expensive cost of oxidizing agents [4,22] and disposal problems of absorption solution [22]. While in oxidation–absorption process, gas phase oxidants, such as hydrogen peroxide [15,16] and ozone [8,17–21], are injected into flue gas first to oxidize NO to $NO_2$ which is highly soluble in water, and then $NO_2$ and $SO_2$ can be removed simultaneously by wet removal process. Ozone has proved to be an efficient gas phase oxidant with advantages of selectivity, high oxidation efficiency, fast oxidation speed and non-pollution decomposition products, etc. [8,17–21]. With respect to the liquid phase absorption of oxidized flue gas, $NO_x$ removal efficiency could reach more than 80% regardless of alkali liquor [8,18,19] or reducing $Na_2S$ [20,21] used.

China has a rich reserve of pyrolusite, of which more than 90% is low-grade with the average content of Mn at 22% [23]. This kind of pyrolusite is not economic in metallurgy not only due to its low content of Mn, but also due to its high operating cost and emissions of pollutants. That is because Mn exists in the form of $MnO_2$

* Corresponding author at: Department of Environmental Science and Engineering, Sichuan University, No. 24 South Section 1, Yihuan Road, Chengdu, Sichuan Province 610065, China. Tel.: +86 28 8546 0916; fax: +86 28 8546 0916.
*E-mail address:* ssjscu@163.com (S.-j. Su).

0304-3894/$ – see front matter © 2011 Elsevier B.V. All rights reserved.
doi:10.1016/j.jhazmat.2011.04.104

which cannot react with $H_2SO_4$ and will be reduced into MnO first by carbon, leading to a huge amount of $CO_2$. However, as an oxidant, $MnO_2$ is able to oxide reducing substance. Because of this function, pyrolusite is commercially used in the field of waste treatment, removing organic matter [24–28] and inorganic matter [29–31] in wastewater and $SO_2$ [32–34] from exhaust gas. A great deal of research on $SO_2$ removal with pyrolusite slurry has been carried out in our earlier work [32–34], with high $SO_2$ removal efficiency and product $MnSO_4{\cdot}H_2O$ of which the quality could reach GB1622286 of China, the industry grade standards. The application of simultaneous removal of $NO_x$ and $SO_2$ with pyrolusite as absorbent has not been reported.

In this work, the objective of the research was to introduce a new process that could obtain the simultaneous removal of $NO_x$ and $SO_2$ from flue gas with resource utilization process of low-grade pyrolusite. Pyrolusite was used as an absorbent in liquid phase to remove $SO_2$ and $NO_x$ simultaneously from flue gas and ozone was injected into flue gas stream to oxidized NO into $NO_2$ to increase solubility of $NO_x$. Reaction mechanism and products during the absorption process were studied, and effects of process parameters on both $NO_x$ and $SO_2$ removal efficiencies and Mn extraction rate were also investigated.

## 2. Theoretical

The simultaneous removal system of $NO_x$ and $SO_2$ consists of two processes: gas-phase oxidation of NO using ozone and absorption of $NO_x$ and $SO_2$ with pyrolusite slurry. Oxidation of NO in gas phase is the first step. When ozone is used as oxidant, $NO_2$ is the predominant oxidation product through reaction (1), although $NO_3$ and $N_2O_5$ are also produced at the same time [8,20,21].

$$NO + O_3 = NO_2 + O_2 \quad (1)$$

The process of simultaneous absorption of $NO_2$ and $SO_2$ with pyrolusite slurry from flue gas is a complex system, which involves gas–liquid–solid mass transfer, chemical reactions in liquid phase, and chemical reactions on pyrolusite surface. Gas dissolution, the process of gas–liquid mass transfer, is the first step of the whole absorption procedure. $SO_2$ dissolves into water and produces $H_2SO_3$, $HSO_3^-$ and $SO_3^{2-}$ by ionization equilibrium, while $NO_2$ can react with water to generate $HNO_2$ and $HNO_3$ [35–38]. At the same time, $O_2$ dissolves into liquid phase in equilibrium with the residual $O_2$ in flue gas. Therefore, $H_2SO_3$, $HSO_3^-$, $SO_3^{2-}$ are the existence forms of S(IV) species, and $NO_2$ and $HNO_2$ are the existence forms of nitrogen species which can react with $O_2$ in liquid phase and $MnO_2$ on pyrolusite surface. The *E*–pH diagrams of Mn–$SO_2$–$NO_x$–$H_2O$ system (Fig. 1) are developed based on thermodynamic data from [39] to analyze reactions that may take place in liquid phase and on pyrolusite surface.

Fig. 1 illustrates that in the Mn–$SO_2$–$NO_x$–$H_2O$ system, oxidation potential of $MnO_2$ and $O_2$ are higher than that of S(IV) species, $NO_2$ and $HNO_2$, indicating that $MnO_2$ and $O_2$ have the potential to oxidize them to $SO_4^{2-}$ and $NO_3^-$, respectively. Accordingly, there are two reaction patterns in the process of $SO_2/NO_x$ removal in flue gas with pyrolusite slurry: (1) $MnO_2$ as oxidant; (2) $O_2$ as oxidant. The exact reactions are presented as follows:

$$MnO_2 + SO_2 = Mn^{2+} + SO_4^{2-} \quad (2)$$

$$SO_2 + H_2O + (1/2)O_2 = 2H^+ + SO_4^{2-} \quad (3)$$

$$MnO_2 + 2NO_2 = Mn^{2+} + 2NO_3^- \quad (4)$$

$$(1/2)O_2 + 2NO_2 + H_2O = 2H^+ + 2NO_3^- \quad (5)$$

$$H^+ + MnO_2 + HNO_2 = Mn^{2+} + NO_3^- + H_2O \quad (6)$$

$$O_2 + 2HNO_2 = 2H^+ + 2NO_3^- \quad (7)$$

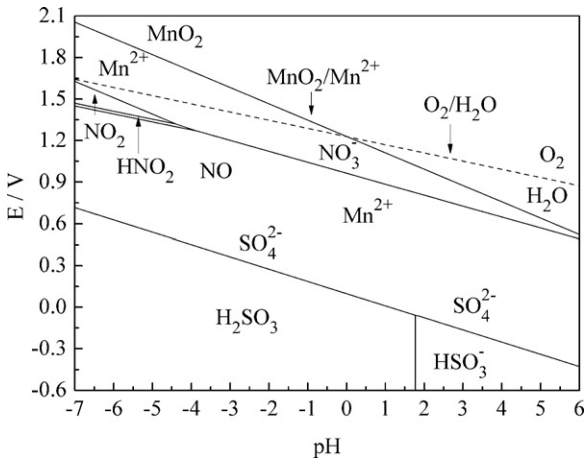


**Fig. 1.** *E*–pH diagram of Mn–$SO_2$–$NO_x$–$H_2O$ system.

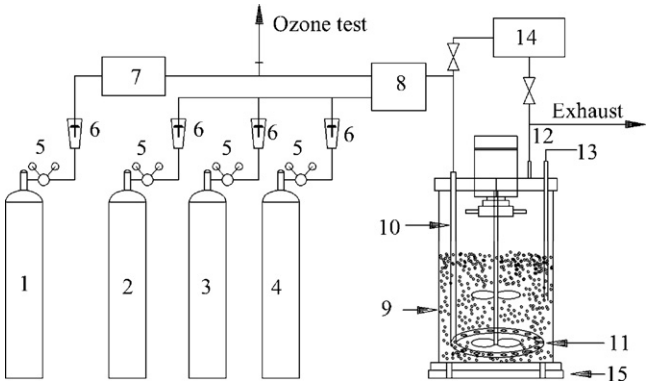


**Fig. 2.** Experimental apparatus and flow. (1). $O_2$ cylinder; (2). $N_2$–$SO_2$ cylinder; (3). $N_2$–NO cylinder; (4). $N_2$ cylinder; (5). relief valve; (6). gas flow meter; (7). ozone generator; (8). ozonizing chamber; (9). agitated bubbling reactor; (10). gas pipe inlet; (11). gas pager; (12). gas pipe outlet; (13). sampling port; (14). gas analyzer; (15). heater

From reactions (2)–(7), it can be seen that under the condition of $MnO_2$ acting as oxidant, $Mn^{2+}$ was produced as reduction product and products of $MnSO_4$ and $Mn(NO_3)_2$ were obtained. In the case of $O_2$ being oxidant, $H_2SO_4$ and $HNO_3$ were obtained.

## 3. Experiments

### 3.1. The experimental system

The experimental system is divided into four parts, i.e., experimental materials supply system, ozone oxidization system, flue gas treatment unit and sampling cum analysis system. A schematic diagram of the experimental set-up is shown in Fig. 2.

#### 3.1.1. Experimental materials supply system

The system mainly consists of simulated flue gas supply and pyrolusite slurry preparation. The simulated flue gas was obtained by the control of mixing different standard gases using gas flow meters and the standard gases include $O_2$, $SO_2$, NO and $N_2$ whose purity were all over 99.9%. Ozone was carried out in an ozone generator with oxygen source (DX-SS1, Harbin Jiujiu Electrochemical Co., Ltd., China), in which output ozone concentration was 0–10 mg/L, and five gears were prepared to change the outlet ozone concentration according to experiment requirement. The feed pyrolusite slurry was prepared by mixing tap water with a required amount

**Table 1**
Compositions of pyrolusite(wt%).

| $MnO_2$ | Fe | Ca | K | Mg | Pb | Ni | Co |
|---|---|---|---|---|---|---|---|
| 27.16 | 3.44 | 3.46 | 1.70 | 0.58 | 0.10 | 0.032 | 0.017 |

**Table 2**
Constant experimental parameters for experiments.

| Experiment parameter | Value |
|---|---|
| Flow rate of gas, L/min | 15 |
| Volume of pyrolusite slurry, L | 5 |
| Concentration of $O_2$, % | 5 |
| Agitator speed, rpm/min | 300 |

of commercial pyrolusite from Guangxi Province, China, and the compositions are shown in Table 1.

### 3.1.2. Ozone oxidization system

The oxidizations of NO and $SO_2$ in flue gas using ozone is taken place in an ozonizing chamber, which was a cylindrical glass tube with inner diameter and length of 5 and 25 cm. Effective volume of ozonizing chamber was calculated to be 500 $cm^3$.

### 3.1.3. Flue gas treatment unit

The absorption of $NO_2$ and $SO_2$ with pyrolusite slurry is taken in a bubbling reactor, which is a well-stirred sealed vessel (ID, 18.5 cm; height, 38 cm) with internal volume of 10 L. Continuous stirring was provided by a mechanical agitator (4 blades disc, turbine type impeller) with a speed of 300 rpm/min. The pH values were detected by METTLER TOLEDO pH combination electrode (405-DPAS-SC-K8S/325). Temperature was proved by an electrical heater at the bottom of reactor and detected by temperature electrode (T817-A-3, Shanghai Precision and Scientific Instrument Co., Ltd., China). There was also an intelligent PID (Proportion Integration Differentiation) temperature control system, which can make sure the error range of temperature to be within 1 °C.

### 3.1.4. Sampling cum analysis system

Negative ions in reactor were analyzed by ion chromatograph (Dionex-ICS-2500). Concentrations of $SO_2$, $NO_x$ and $O_2$ in inlet and outlet flue gas were detected by a set of online gas analyzer (SMC-9021, Sick Maihak Co., Ltd., Beijing, China). Concentrations of manganese in both liquid samples and pyrolusite were determined by atomic absorption spectrometer (AA7000 Institute of Eastwest Electronic Technology of Beijing, China). Ozone concentration was measured by the iodometric procedure (Ozone Standards Committee Method), in which ozone was absorbed by neutral solution of potassium iodine and then the solution was acidified and the liberated iodine was drawn of by the sodium thiosulphate [40].Experiment parameters

In our research, flue gas was oxidized by ozone continuously in gas phase and then absorbed by pyrolusite slurry in liquid phase under semi-batch condition. Some experiment parameters, including inlet ozone concentration, inlet NO concentration, reaction temperature and the pyrolusite slurry concentration, were changed in order to examine their effects on $NO_x/SO_2$ removal efficiency and Mn extraction rate. The constant experimental parameters for the whole experiment were displayed in Table 2.

With regard to an oxidation–absorption process for $NO_x$ and $SO_2$ removal combined ozone with pyrolusite slurry, the main parameters considered include oxidation rate of $NO/SO_2$, removal efficiency of $NO_x/SO_2$ and Mn extraction rate. In order to clearly explain analytical methods for these parameters, the flue gas before oxidized was called “inlet flue gas” and the flue gas oxidized by ozone but before absorbed was called “oxidized flue gas” and the flue gas absorbed was called “oulet flue gas”.

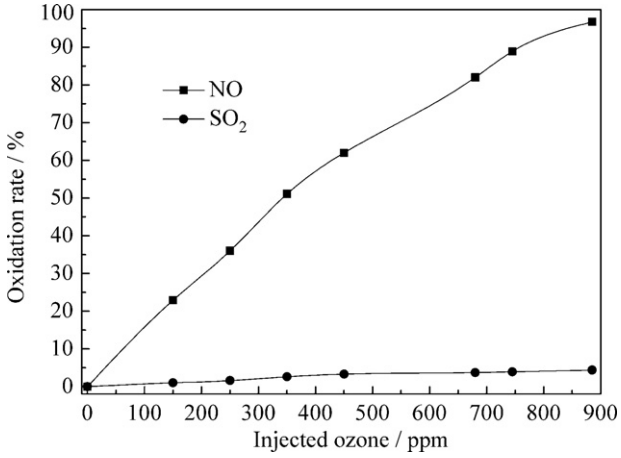


**Fig. 3.** Variations of oxidation rate of NO and $SO_2$ with injected ozone concentration (concentration of NO, 1500 ppm; reaction temperature, 25 °C).

The oxidation rate of $NO/SO_2$ was analyzed as follows:

$$\text{Oxidization rate } (\%) = \frac{C_{\text{inlet}} - C_{\text{oxidized}}}{C_{\text{inlet}}} \times 100 \quad (8)$$

where, $C_{\text{inlet}}$ is the concentration of $NO/SO_2$ in inlet flue gas, ppm; $C_{\text{oxidized}}$ is the concentration of $NO/SO_2$ in oxidized flue gas, ppm.

The removal efficiency of $NO_x/SO_2$ was analyzed as follows:

$$\text{Removal efficiency } (\%) = \frac{C_{\text{inlet}} - C_{\text{outlet}}}{C_{\text{inlet}}} \times 100 \quad (9)$$

where, $C_{\text{inlet}}$ is the concentration of $NO_x/SO_2$ in inlet flue gas, ppm; $C_{\text{outlet}}$ is the concentration of $NO_x/SO_2$ in outlet flue gas, ppm

Equation for expressing manganese extraction rate as follows:

$$\text{Mn extraction rate } (\%) = \frac{m_{\text{liquidoid}}}{m_{\text{total}}} \times 100 \quad (10)$$

where, $m_{\text{liquidoid}}$ is the net mass of $Mn^{2+}$ in liquid phase in reactor, g; $m_{\text{total}}$ is the net mass of Mn in liquid and pyrolusite, g.

## 4. Results and discussion

### 4.1. Oxidations of NO and $SO_2$ using ozone in gas phase

The oxidation efficiency of ozone, which was served as a gas-phase oxidant, determined the $NO_x$ existing form in flue gas, as a result of affecting the $NO_x$ removal efficiency. This thesis examined the effect of ozone concentration on oxidation rates of NO and $SO_2$. The results were briefly summarized in Fig. 3.

Fig. 3 showed that ozone could oxidize NO in flue gas contrapuntally and effectively, and the NO oxidation rate went up with the ozone concentration linearly. When injected ozone was at about 750 and 900 ppm, the NO oxidation rate turned out to be 88% and 97%, respectively. But ozone had little impact on $SO_2$ oxidation, that is, the oxidation rate of $SO_2$ was less than 5% as injected ozone was at about 900 ppm. The selectivity of ozone on NO oxidation could save the oxidant cost.

### 4.2. Reaction mechanism and products during absorption process

#### 4.2.1. Effects of ozone and pyrolusite on $NO_x$ removal efficiency

The research studied the effect of ozone and pyrolusite slurry on $NO_x$ removal efficiency in a wet process. Variations of pH value, output NO concentration and $NO_x$ removal efficiency were displayed

**Table 3**
Concentrations of species in liquid phase.

| | pH | $NO_3^-$/mol $L^{-1}$ | $NO_2^-$/mol $L^{-1}$ | $Mn^{2+}$/mol $L^{-1}$ |
|---|---|---|---|---|
| NO + pyrolusite(10 g/L) | 3.67 | 0.025 | 0.0040 | 0.0089 |
| NO + ozone(1800 ppm) + running water | 0.95 | 0.1203 | 0.0107 | – |
| NO + ozone(1800 ppm) + pyrolusite(10 g/L) | 1.14 | 0.1384 | 0 | 0.0280 |

Concentration of NO, 1500 ppm; reaction temperature, 25 °C.

**Table 4**
Relationship of total amount between $SO_2/NO_x$ removed from flue gas and $SO_4^{2-}$, $NO_3^-$ in liquid phase.

| Nitrogen species | | | Sulphur species | | |
|---|---|---|---|---|---|
| $NO_x$ removed from flue gas ($A_1$)/mol | $NO_3^-$ in liquid phase ($B_1$)/mol | Ratio of $A_1/B_1$ | $SO_2$ removed from flue gas ($A_2$)/mol | $SO_4^{2-}$ in liquid phase ($B_2$)/mol | Ratio of $A_2/B_2$ |
| 0.0623 | 0.0591 | 1.054:1 | 0.2172 | 0.209 | 1.039: 1 |

Concentration of NO, 750 ppm; concentration of $SO_2$, 2000 ppm; concentration of ozone, 900 ppm; concentration of pyrolusite, 40 g/L; reaction temperature, 25 °C.

in Fig. 4. Concentrations of species in liquid phase at the end of reaction were exhibited in Table 3.

As shown in Fig. 4 and Table 3, when there was no ozone in the system, $NO_x$ removal efficiency was around 15% (Fig. 4(b)), and the manganese concentration in liquid phase appeared to be quite low (Table 3). This was mainly due to the fact that NO is insoluble and the reaction was controlled by gas–liquid mass transfer [41]. Reversely when 1800 ppm ozone was injected into system, $NO_x$ removal efficiency increased to about 75% (Fig. 4(b)). The reason was that NO could be oxidized into $NO_2$, which is more soluble than NO. If the absorbent was water, the output NO concentration increased from 25 to 152 ppm with reaction time (Fig. 4(a)) and $NO_x$ removal efficiency decreased (Fig. 4(b)). The main reason was that a great amount of $HNO_3$ produced in the system made pH value drop to 0.95 (Table 3), resulting in the decomposition of $HNO_2$. If pyrolusite slurry was used as absorbent, output NO only increased from 25 to 52 ppm (Fig. 4(a)) and $NO_x$ removal efficiency could still reach achieve 70% (Fig. 4(b)), and no $HNO_2$ was detected in liquid phase (Table 3). This illustrated that $MnO_2$ in pyrolusite slurry could consume $HNO_2$ and $NO_2$ immediately, preventing $HNO_2$ from decomposition and enhancing $NO_x$ removal efficiency.

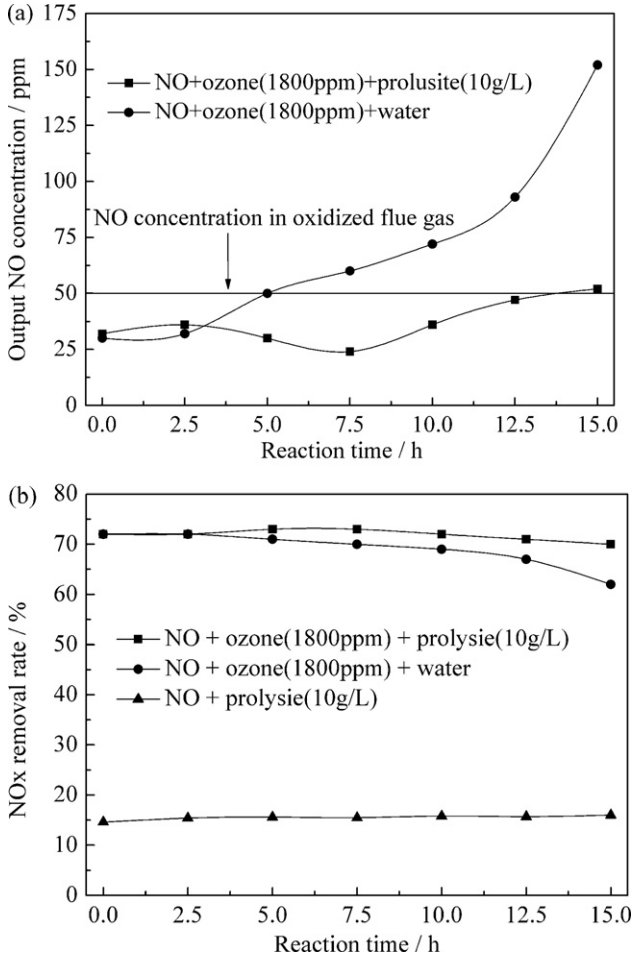


**Fig. 4.** (a) Variations of Output NO concentration and (b) $NO_x$ removal efficiencies in different removal process (concentration of NO, 1500 ppm; reaction temperature, 25 °C).

*4.2.2. Simultaneous absorption of $NO_x$ and $SO_2$ with pyrolusite slurry combined with gas-phase oxidation of NO using ozone*

NO in flue gas was oxidized into $NO_2$ by ozone in gas phase. The oxidized flue gas was continuously entered into reactor filled with a certain volume and concentration of pyrolusite slurry. Variations of $SO_2/NO_x$ removal efficiency, pH value and Mn extraction rate with reaction time were displayed in Fig. 5. The relationship of total amount between $SO_2$ and $NO_x$ removed from flue gas and $SO_4^{2-}$, $NO_3^-$ in liquid phase were all listed in Table 4.

Results collected in Fig. 5(a) indicated that Mn extraction rate increased and pH decreased gradually with reaction time. In the former 8 h, $SO_2$ and $NO_x$ removal efficiencies remained relatively stable at 100% and 74% (Fig. 5(b)). While 8 h later, pH value was lower than 1.0 (Fig. 5(a)) and $SO_2$ removal efficiency began to decrease and output NO concentration came to increase (Fig. 5(b)). When reaction lasted for 14 h, Mn extraction rate arrived at 92% and pH value decreased to 0.68 (Fig. 5(a)). Furthermore, output NO reached to 45 ppm, $SO_2$ and $NO_x$ removal efficiencies were reduced to 79% and 70% (Fig. 5(b)), respectively.

According to mechanism discussed in section 1, S(IV) species, $NO_2$ and $HNO_2$ in liquid phase were oxidized by both of $MnO_2$ and $O_2$. With the gradual reduction of $MnO_2$ in the liquid phase, the system oxidation would be diminished, leading to the decrease of $SO_2$ and $NO_x$ removal efficiencies. On the other hand, through reactions (3), (5) and (7), $H_2SO_4$ and $HNO_3$ were produced and led to pH value decreasing, the low solubility of $SO_2$ and the decomposition of $HNO_2$ in liquid phase, which also contributed to the decreasing $SO_2$ and $NO_x$ removal efficiencies.

Table 4 showed that both ratios of total amount of $NO_x/SO_2$ removed from flue gas to $NO_3^-/SO_4^{2-}$ in liquid phase were about 1:1, indicating that the products of $SO_2$ and $NO_x$ removal process were $SO_4^{2-}$ and $NO_3^-$, without other valence states of sulphur species, nitrogen species or sulphur–nitrogen compounds produced. This was owing to the fact that $H_2SO_4$ and $HNO_3$ produced in system resulted in the lower pH value, while the oxidation poten-

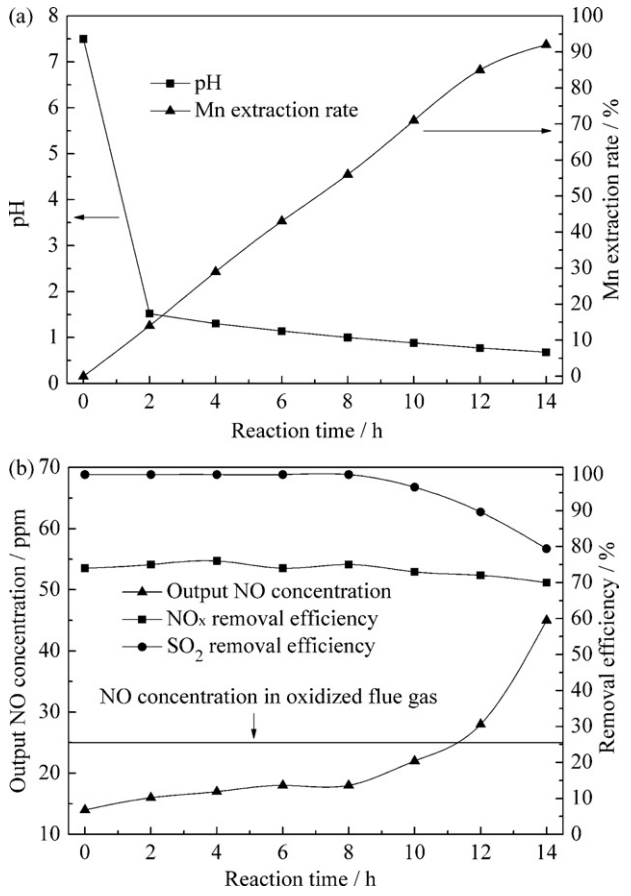


**Fig. 5.** Parameter variation characters of $SO_2/NO_x$ removal system with pyrolusite slurry (concentration of NO, 750 ppm; concentration of $SO_2$, 2000 ppm; concentration of ozone, 900 ppm; concentration of pyrolusite, 40 g/L; reaction temperature, 25 °C). (a) Variations of pH and output NO concentration with reaction time. (b) Variations of $SO_2/NO_x$ removal efficiency and Mn extraction rate with reaction time.

tial of $MnO_2$ went up with lower pH, thus a strong oxidation system was formed to oxidize the S(IV) species, $NO_2$ and $HNO_2$ in liquid phase into $SO_4^{2-}$ and $NO_3^-$, respectively.

The variations of various parameters in system showed that Mn extraction rate increased and pH decreased with reaction time, while $SO_2$ and $NO_x$ removal efficiencies decreased with the increasing Mn extraction rate and decreasing pH. Therefore, in order to obtain satisfying $NO_x$ removal efficiency and Mn extraction rate with high $SO_2$ removal efficiency at the same time, we set the $SO_2$ removal efficiency at 90% as the end of semi-batch reaction. The effects of temperature and concentrations of ozone, inlet NO and pyrolusite on $NO_x$ removal efficiency and Mn extraction rate were discussed on the base of $SO_2$ removal efficiency at 90%.

### 4.3. Effect of ozone concentration on $NO_x$ removal efficiency and Mn extraction rate

Ozone concentration determined NO oxidation rate and affected $NO_x$ absorption efficiency. The effects of injection ozone concentration on $NO_x$ removal efficiency and Mn extraction rate were studied. The experimental results were shown in Fig. 6.

Fig. 6 indicated that the Mn extraction rate maintained at about 85%, while $NO_x$ removal efficiency increased from 15% to 75% when the ozone concentration rose from 0 to 900 ppm. This is mainly due to the fact that the increasing injection ozone concentration increased $NO_x$ oxidation rate and accelerated the $NO_x$ dissolution, which were helpful for the removal efficiency.

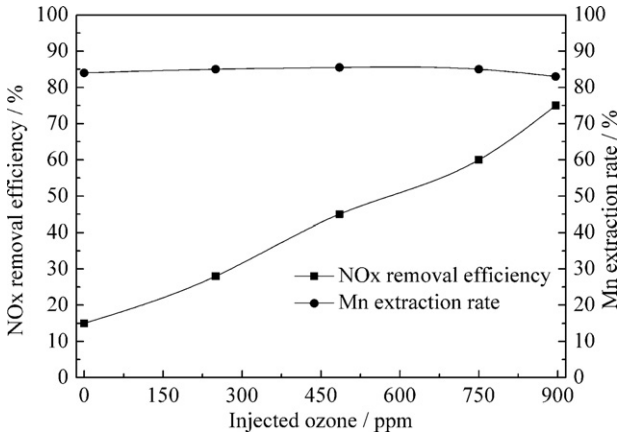


**Fig. 6.** Variations of $NO_x$ removal efficiency and Mn extraction rate with injected ozone concentration (concentration of NO, 750 ppm; concentration of $SO_2$, 2000 ppm; concentration of pyrolusite, 40 g/L; reaction temperature, 25 °C).

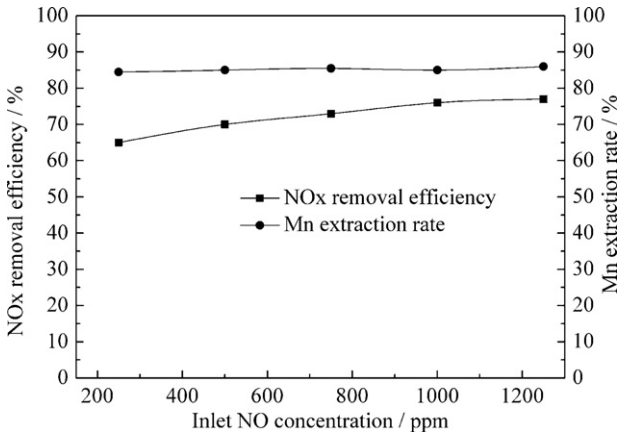


**Fig. 7.** Variations of $NO_x$ removal efficiency and Mn extraction rate with inlet NO concentration (concentration of $SO_2$, 2000 ppm; concentration of pyrolusite, 40 g/L; reaction temperature, 25 °C).

### 4.4. Effect of NO concentration on $NO_x$ removal efficiency and Mn extraction rate

Effect of inlet NO concentration on the simultaneous removal of $SO_2$ and $NO_x$ was investigated and results were displayed in Fig. 7. Molar ratio of ozone to NO remained at 1.2:1.

As shown in Fig. 7, inlet NO concentration had trivial effect on Mn extraction rate. $NO_x$ removal efficiency increased slightly when inlet NO concentration increased from 250 to 1250 ppm, The reason might be that the gas–liquid mass transfer rate of $NO_x$ was proportional to the concentration driving force according to film theory and the increase of gas partial pressure increased the concentration driving force between gas phase and liquid phase [11]. As a result, the gas–liquid mass transfer rate of $NO_x$ was enhanced.

### 4.5. Effects of temperature on $NO_x$ removal efficiency and Mn extraction rate

Temperature was changed from about 30 °C to 70 °C in order to examine its effect on $NO_x$ removal efficiency and Mn extraction rate.

Fig. 8 indicated that the Mn extraction rate increased first and then dropped with the rise of reaction temperature. The highest Mn extraction rate of 86% was achieved at 50 °C. $NO_x$ removal efficiency remained stable at 74% with the increase of reaction temperature from 20 °C to 40 °C, but decreased when the flue gas temperature

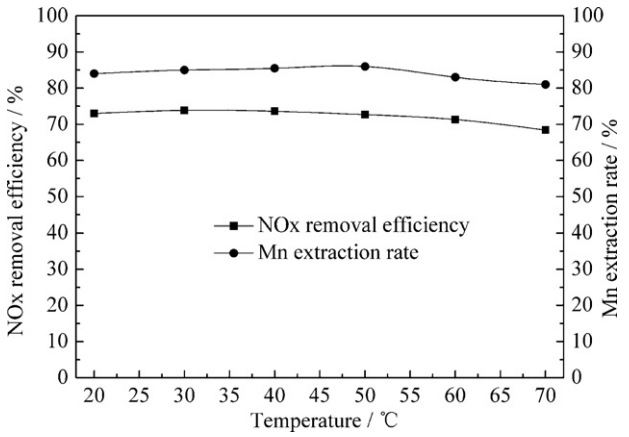


**Fig. 8.** Variations of $NO_x$ removal efficiency and Mn extraction rate with temperature (concentration of NO, 750 ppm; concentration of $SO_2$, 2000 ppm; concentration of ozone, 900 ppm; concentration of pyrolusite, 40 g/L).

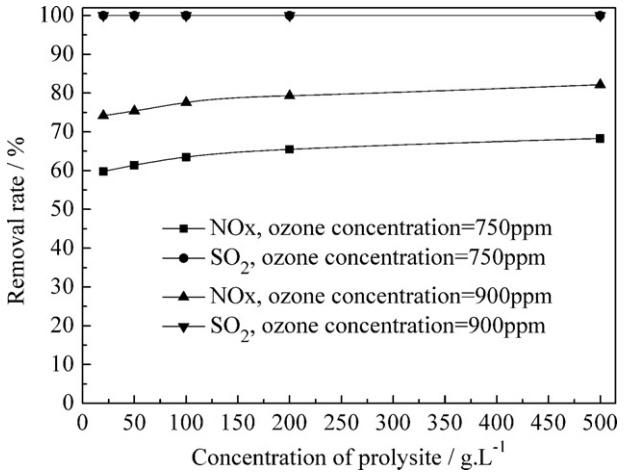


**Fig. 9.** Variations of $SO_2/NO_x$ removal efficiency with pyrolusite concentration (concentration of NO, 750 ppm; concentration of $SO_2$, 2000 ppm; reaction temperature, 25 °C).

exceeded 40 °C. It could be explained from two aspects positively or negatively. On one hand, the increase of the temperature could enhance mass transfer coefficient of $NO_x$ and $SO_2$ and promoted the reaction rate [11,32]. On the other hand, with the rise of the reaction temperature, the decomposition of $HNO_2$ was promoted, and the absorption of $SO_2$ was also inhibited because of the reduction of the solubility [32]. When the positive effect was greater than the negative effect, the $NO_x$ removal efficiency and Mn extraction rate increased, otherwise, they decreased.

### 4.6. Effect of pyrolusite concentration on simultaneous removal of $SO_2$ and $NO_x$

Some experiments were also performed to investigate the effect of pyrolusite concentration on $SO_2/NO_x$ removal efficiency.

According to Fig. 9, $SO_2$ removal efficiency was nearly 100% and $NO_x$ removal efficiency improved with higher pyrolusite concentration, when pyrolusite concentration was kept at 500 g/L and $NO_x$ removal efficiency reached 82%. This is due to the fact that pyrolusite dispersed throughout aqueous phase as solid particles, which was favorable to increase gas–liquid interfacial area by breaking gas bubbles and preventing its combination, enhancing gas–liquid mass transfer rate of $NO_x$ [42,43].

## 5. Conclusions

Simultaneous absorption process of $NO_x$ and $SO_2$ from flue gas with pyrolusite slurry combined with gas-phase oxidation of NO using ozone was investigated. Ozone could oxidize NO to $NO_2$ with selectivity and high efficiency, furthermore, $MnO_2$ in pyrolusite slurry could oxidize $SO_2$ and $NO_2$ into $MnSO_4$ and $Mn(NO_3)_2$ in liquid phase, respectively. Temperature and concentrations of injected ozone and inlet NO had little impact on both $SO_2$ removal efficiency and Mn extraction rate. Mn extraction rate remained steady at around 80–86% when $SO_2$ removal efficiency dropped to 90%. $NO_x$ removal efficiency reached 82% when inlet NO at 750 ppm, injected ozone at 900 ppm, concentration of pyrolusite at 500 g/L and temperature at 25 °C.

The new process employed low-grade pyrolusite as an absorbent to remove $NO_x$ and $SO_2$ from flue gas and obtained the mixed solution of $Mn(NO_3)_2$ and $MnSO_4$ economically in the mean time, which controlled the pollution of $NO_x$ and $SO_2$ and realized the resource utilization process. In this way, the new process has good potential to be put into practice.

## Acknowledgement

This project is founded by the National High Technology Research and Development Program of China (863 Program), 2008AA06Z316.

## References

[1] H. Chu, T.W. Chien, S.Y. Li, Simultaneous absorption of $SO_2$ and NO from flue gas with $KMnO_4$/NaOH solutions, Sci. Total Environ. 275 (2001) 127–135.
[2] V. Ramanathan, Y. Feng, Air pollution, greenhouse gases and climate change: global and regional perspectives, Atmos. Environ. 43 (2009) 37–50.
[3] H.S. Zhu, Y.P. Mao, X.J. Yang, et al., Simultaneous absorption of NO and $SO_2$ into $Fe^{II}$–EDTA solution coupled with the $Fe^{II}$–EDTA regeneration catalyzed by activated carbon, Sep. Purif. Technol. 74 (2010) 1–6.
[4] X. Long, Z. Xin, M. Chen, W. Li, W. Xiao, W. Yuan, Kinetics for the simultaneous removal of NO and $SO_2$ with cobalt ethylenediamine solution, Sep. Purif. Technol. 58 (2008) 328–334.
[5] D.S. Jin, B.R. Deshwal, Y.S. Park, H.K. Lee, Simultaneous removal of $SO_2$ and NO by wet scrubbing using aqueous chlorine dioxide solution, J. Hazard Mater. B135 (2006) 412–417.
[6] X. She, M. Flytzani-Stephanopoulos, Activity and stability of Ag–alumina for the selective catalytic reduction of $NO_x$ with methane in high-content $SO_2$ gas streams, Catal. Today 127 (2007) 207–218.
[7] L. Wang, W. Zhao, Z. Wu, Simultaneous absorption of NO and $SO_2$ by FeII–EDTA combined with $Na_2SO_3$ solution, Chem. Eng. J. 132 (2007) 227–232.
[8] Z. Wang, J. Zhou, Y. Zhu, Z. Wen, J. Liu, K. Cen, Simultaneous removal of $NO_x$, $SO_2$ and Hg in nitrogen flow in a narrow reactor by ozone injection: experimental results, Fuel Process. Technol. 88 (2007) 817–823.
[9] Y. Zhao, P. Xu, D. Fu, J. Huang, H. Yu, Experimental study on simultaneous desulfurization and denitrification based on highly active absorbent, J. Environ. Sci. China 18 (2006) 281–286.
[10] T.W. Chien, H. Chu, Removal of $SO_2$ and NO from flue gas by wet scrubbing using an aqueous $NaClO_2$ solution, J. Hazard Mater. 80 (2000) 43–57.
[11] Y. Zhao, T. Guo, Z. Chen, Y. Du, Simultaneous removal of $SO_2$ and NO using M/$NaClO_2$ complex absorbent, Chem. Eng. J. 160 (2010) 42–47.
[12] T.W. Chien, H. Chu, H.T. Hsueh, Kinetic study on absorption of $SO_2$ and $NO_x$ with acidic $NaClO_2$ solutions using the spraying column, J. Environ. Eng. ASCE 129 (2003) 967–974.
[13] Y. Liu, J. Zhang, C. Sheng, Y. Zhang, L. Zhao, Simultaneous removal of NO and $SO_2$ from coal-fired flue gas by UV/$H_2O_2$ advanced oxidation process, Chem. Eng. J. 162 (2010) 1006–1011.
[14] H. Chu, S.Y. Li, T.W. Chien, The absorption kinetics of NO from flue gas in a stirred tank reactor with $KMnO_4$/NaOH solutions, J. Environ. Sci. Health A 33 (1998) 801–827.
[15] J.M. Kasper, C.A. Clausen III, C.D. Cooper, Control of nitrogen oxide emissions by hydrogen peroxide enhanced gas-phase oxidation of nitric oxide, J. Air Waste Manage. Assoc. 46 (1996) 127–133.
[16] C.D. Cooper, C.A. Clausen, L. Pettey, et al., Investigation of UV enhanced $H_2O_2$ oxidation of $NO_x$ emissions, Environ. Eng. 128 (2002) 68–72.
[17] Y. Fu, U.M. Diwekar, Cost effective environmental control technology for utilities, Adv. Environ. Res. 8 (2003) 173–196.
[18] Z.H. Wang, B. Li, A. Ehn, Z.W. Sun, Z.S. Li, J. Bood, M. Aldén, K.F. Cen, Investigation of flue-gas treatment with $O_3$ injection using NO and $NO_2$ planar laser-induced fluorescence, Fuel 89 (2010) 2346–2352.

[19] Z. Wang, J. Zhou, J. Fan, K. Cen, Direct numerical simulation of ozone injection technology for $NO_x$ control in flue gas, Energy Fuel 20 (2006) 2432–2438.
[20] Y.S. Mok, H.J. Lee, Removal of sulfur dioxide and nitrogen oxides by using ozone injection and absorption–reduction technology, Fuel Process Technol. 87 (2006) 591–597.
[21] Y.S. Mok, Absorption–reduction technique assisted by ozone injection and sodium sulfide for $NO_x$ removal from exhaust gas, Chem. Eng. J. 118 (2006) 63–67.
[22] K. Chandrasekara Pillai, S.J. Chung, T. Raju, I. Moon, Experimental aspects of combined $NO_x$ and $SO_2$ removal from flue-gas mixture in an integrated wet scrubber-electrochemical cell system, Chemosphere 76 (2009) 657–664.
[23] Z.Z. Tan, G.G. Mei, W.J. Li, Hydrometallurgy, Central South University Press, Changsha, 2004.
[24] F.B. Li, C.S. Liu, C.H. Liang, et al., The oxidative degradation of 2-mercaptobenzothiazole at the interface of β-$MnO_2$ and water, J. Hazard Mater. 154 (2008) 1098–1105.
[25] H. Zhang, C. Huang, Oxidative transformation of fluoroquinolone antibacterial agents and structurally related amines by manganese oxide, Environ. Sci. Technol. 39 (2005) 4474–4483.
[26] R.A. Petrie, P.R. Grossl, R.C. Sims, Oxidation of pentachlorophenol in manganese oxide suspensions under controlled $E_h$ and pH environments, Environ. Sci. Technol. 36 (2002) 3744–3748.
[27] P.S. Nico, R.J. Zasoski, Mn(III) center availability as a rate controlling factor in the oxidation of phenol and sulfide on δ-$MnO_2$, Environ. Sci. Technol. 35 (2001) 3338–3343.
[28] H. Zhang, C. Huang, Reactivity and transformation of antibacterial N oxides in the presence of manganese oxide, Environ. Sci. Technol. 39 (2005) 593–601.
[29] S.E. Fendorf, R.J. Zasoski, Chromium(III) oxidation by δ-$MnO_2$.1. Characterization, Environ. Sci. Technol. 26 (1992) 79–85.
[30] X.H. Feng, Y.Q. Zu, W.F. Tan, et al., Arsenite oxidation by three types of manganese oxides, J. Environ. Sci. 18 (2006) 292–298.
[31] X.J. Li, C.S. Liu, F.B. Li, et al., The oxidative transformation of sodium arsenite at the interface of α-$MnO_2$ and water, J. Hazard Mater. 173 (2010) 675–6381.
[32] S.J. Shu, X.F. Zhu, Y.J. Liu, et al., A pilot-scale jet bubbling reactor for wet flue gas desulfurization with pyrolusite, J. Environ. Sci. China 17 (2005) 827–831.
[33] J.D. Zhao, S.J. Su, N.S. Ai, et al., Modelling flue gas desulfurization using pyrolusite pulp in a jet bubbling reactor, Mater. Sci. Forum 610–613 (2009) 85–96.
[34] J.D. Zhao, S.J. Su, X.F. Zhu, et al., Experimental study on macro-kinetics of flue gas desulfurization using pyrolusite pulp by a double magnetic stirred reactor, Mater. Sci. Forum 610–613 (2009) 32–40.
[35] D. Thomas, J. Vanderschuren, The absorption–oxidation of $NO_x$ with hydrogen peroxide for the treatment of tail gases, Chem. Eng. Sci. 51 (1996) 2649–2654.
[36] Y. Li, Y.Z. Liu, L.Y. Zhang, et al., Absorption of $NO_x$ into nitric acid solution in rotating packed bed, Chin. J. Chem. Eng. 18 (2010) 244–248.
[37] D. Thomas, J. Vanderschuren, Analysis and prediction of the liquid phase composition for the absorption of nitrogen oxides into aqueous solutions, Sep. Purif. Technol. 18 (2000) 37–45.
[38] J.A. Patwardhan, M.P. Pradhan, J.B. Joshi, Simulation of $NO_x$ gas absorption under adiabatic condition and comparison with plant data, Chem. Eng. Sci. 57 (2002) 4831–4844.
[39] Speight, G. James, Lange's Handbook of Chemistry, 16th ed., McGraw-Hill, New York, 2004.
[40] IOA (International Ozone Association), Iodometric Method for The Determination of Ozone in A Process Gas, Quality Assurance Committee, Revised Standardized Procedure 001/96, 1996.
[41] B.R. Deshwal, H.K. Lee, Mass transfer in the absorption of $SO_2$ and $NO_x$ using aqueous euchlorine scrubbing solution, J. Environ. Sci. 21 (2009) 155–161.
[42] A.M. Nienow, M. Kone, W. Bujuski, Studies on the three-phase mixing: a review and recent results, Chem. Eng. Res. Des. 64 (1986) 35–42.
[43] M. Schmitz, A. Steiff, Gas/liquid interfacial area per unit volume and volumetric mass transfer coefficient in stirred slurry reactors, Chem. Eng. Technol. 10 (1987) 204–215.